Electronic Supporting Information

Formation of thin and continuous MOF membrane with 2-D MOF nanosheets as seeds via Layer-by-Layer growth

Yingnan Ma[a], Zhaopeng Dong[a], Meng You[a] , Yufeng Zhang[a], Xianshe Feng[b], Xiaohua Ma [a*], Jianqiang Meng[a*]

a. State Key Laboratory of Separation Membranes and Membrane Processes, Tianjin Polytechnic University, Tianjin 300387, PR China

b. Department of Chemical Engineering, University of Waterloo, Waterloo, Ontario, Canada N2L 3G1

*Corresponding author. Tel.: +86 22 83955386; fax: +86 22 83955055

E-mail addresses: jianqiang.meng@hotmail.com, jianqiang.meng@tjpu.edu.cn;

 xhuama@126.com

† Footnotes relating to the title and/or authors should appear here.

Content

1. Materials and methods

1.1 Chemicals and materials

Polyacrylonitrile (PAN) membrane (GC-UF0503, M_w=100000) was purchased from SEPRO (USA), and the PAN UF membrane is a copolymer of PAN and PMA (Phorbol-12-myristate-13-acetate). N-N-dimethylformamide (DMF), sodium hydroxide (NaOH), benzimidazole (bim, $C_7H_6N_2$>99%), 2-N-methylimidazole (HMIm, $C_4H_6N_2$>99%) were purchased from Kermel (Tianjin, China). Zinc nitrate hexahydrate ($Zn(NO_3)_2 \cdot 6H_2O$, >98%), methanol, propyl alcohol were purchased from Sigma-Aldrich. All the chemicals were used as received without further purification.

1.2 Characterization methods

1.2.1 Surface X-ray powder diffraction (XRD) and Fourier transform infrared spectroscopy (FTIR) analyses

The X-ray diffraction (XRD) spectra were obtained using a D8 Discover X-ray diffraction analysis device from Bruker (Germany), with a Cu K_α (λ=0.1542nm) anode from 5 to 40 (2θ) with a 0.001° step size.

The Fourier transform infrared spectroscopy (FT-IR) analysis was carried out with a Nicolet iS50 Fourier transform infrared spectrometer from Thermo Fisher Scientific (China) with a spectral range of 7800-350 cm^{-1}. For both the XRD and FTIR tests, the samples were dried under a vacuum for 48 h beforehand.

1.2.2 Scanning electron microscopic (SEM) images

Scanning electron microscopic (SEM) images were taken on a Gemini SEM500 high resolution scanning electron microscope from ZEISS (Germany). The samples were horizontally attached to an aluminum support for imaging of the membrane surface. As for cross-sectional imaging, the samples were frozen and fractured with liquid nitrogen. All samples were dried at 50°C overnight.

1.2.3 Transmission Electron Microscope (TEM) and energy dispersive X-ray spectroscopy (EDX)

Transmission Electron Microscope (TEM) images were taken on a JEM-2100F Transmission Electron Microscope from Joel (Japan), and the samples were placed in 100 mL of mixed solvent of methanol and n-propanol (1:1) and sonicated for 5 h. Energy dispersive spectroscopy (EDX) maps of the main elements were obtained by scanning an area of 60 mm^2 with an energy dispersive spectroscopy OCTANE SUPER from EDAX (USA). The mapping was carried out a total of 8 times, 2 minutes for each sample. The distribution of Zn element was then examined.

1.2.4 Water contact angles (WCA)

Water contact angles (WCA) of membranes were tested by a contact angle meter (Kruss CM3250-DS3210, Germany). A droplet of deionized water (2 μL) was dropped on the NFM surface and analyzed by the Circle-

Fitting method using a drop shape analysis software.

2. Experimental section and discussion

2.1 Synthesis of $Zn_2(bim)_4$ via hydrothermal transformation of ZIF-7 particles

The $Zn_2(bim)_4$ nanosheets were prepared from layered $Zn_2(bim)_4$ precursors which could be obtained by ZIF-7 particles[24]. First, ZIF-7 particles were synthesized using a solvothermal protocol, 3.025 g (10 mmol) of $Zn(NO_3)_2\cdot 6H_2O$ and 7.695 g (65 mmol) of benzimidazole being added in 400 mL DMF. The molar ratio of Zn^{2+}/bim/DMF was 0.154:1:80. After being stirred for 2 h, the solution was kept at 25 °C for 72 h for the growth of ZIF-7 crystals. The ZIF-7 particles were recovered by centrifugation and thoroughly washed with methanol (3 times) and centrifugal collection. The wet product was dried at 50 °C for 12 h and then dried at 120 °C for 48 h in a vacuum oven. As a hydrothermal transformation process, the obtained MOF crystals (0.5 g) were dispersed in 100 mL of distilled water, then boiled and refluxed at 100 °C for 24 h.

2.2 Exfoliation of $Zn_2(bim)_4$ precursors toward 2-D $Zn_2(bim)_4$ nanosheets

The $Zn_2(bim)_4$ product was collected by centrifugation, washed with distilled water and methanol, then dried at 50 °C for 12 h. The $Zn_2(bim)_4$ powder（0.01 g）was then dispersed in 100 mL mixture solvent of methanol and n-propanol (1:1) and sonicated for 5 h. After three days of standing, MOF nanosheets formed colloidal suspension in supernatant. During the exfoliation process, small methanol molecules intercalate into the interlayer space for breaking the interlayer interactions to form nanosheets, while n-propanol adsorbs onto the obtained nanosheets and prevent the nanosheets restacking together to form bulky precursors[24]. The sediment was removed and the MOF nanosheets were collected by centrifuging at 20000 rpm for 60 min. Finally, the product was dried at 50 °C in a vacuum oven for 12 h.

2.3 Preparation of the ZIF-8 composite membrane

The PAN membranes were first hydrolyzed by treating 2 mol/L NaOH for 20 min at 80 °C [26] to introduce the carboxyl groups which can link ZIF-7 nanosheets by coordinating with Zn ions. Then the hydrolytic PAN membranes were washed by pure water and then oxalic acid was added until the pH value becomes neutral. Next we deposited $Zn_2(bim)_4$ nanosheets on PAN membrane by vacuum filtration method, and then the substrate was washed by methanol to remove the 2-D MOF nanosheets attached by the Van der Waals' force. By this facile method, we obtained the $Zn_2(bim)_4$ nanosheets/PAN membranes.

The ZIF-8 composite membrane was prepared by a L-b-L method on the $Zn_2(bim)_4$ nanosheets /PAN substrate. The substrate was first fixed on a glass plate to ensure ZIF-8 layer growth only on one side, then immersed in 2-N-methylimidazole (6.6 g ,80 mmol)/methanol (30 mL) for 15 mins, washed by methanol for 30 min, and finally the membrane was immersed in 0.6 g of $Zn(NO_3)_2 \cdot 6H_2O$ (2mmol)/30 mL of methanol for 15 min. This operation was repeated 6-10 times until a continuous ZIF-8 layer formed.
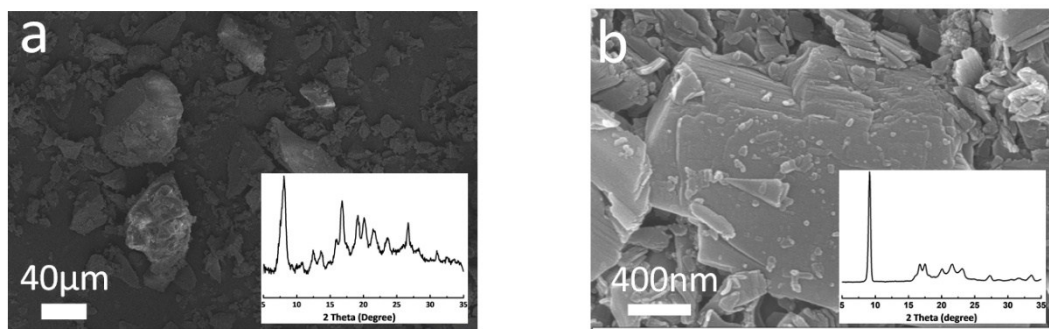

Fig. S1. Scanning electron microscopic (SEM) images of ZIF-7 crystals (a) and layered $Zn_2(bim)_4$ (b)

It can be observed that the morphology of ZIF-7 crystals changed from 3-D structure (Fig. S1a) to layered $Zn_2(bim)_4$ (Fig. S1b) crystals after the hydrothermal transformation. In the layered structure, each Zn ion is connected by four benzimidazole ligands, at the same time, each benzimidazole links two Zn ions by a bis-monodentate connectivity. In this structure, each $Zn_2(bim)_4$ layer is oriented normal to the c axis and stacks together by weak Van der Waals interactions[24].
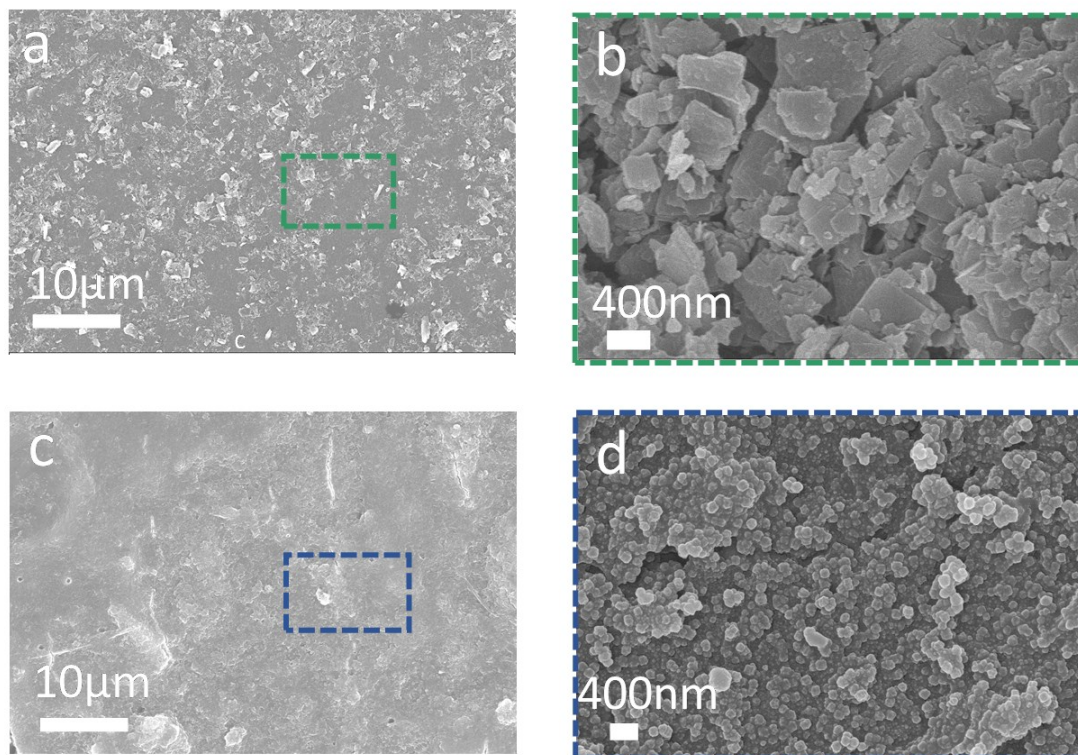
Fig. S2. SEM imagines of ZIF-8 composite membrane after 1-cycle L-b-L growth (a,b) and 6-cycles L-b-L growth (c,d).

In order to explore the influence of L-b-L growth frequency on membrane morphology, ZIF-8 composite membrane after less L-b-L growth cycle were characterized by SEM too. As is shown in Fig. S2a,b, for 1 cycle L-b-L growth, MOF crystals started to grow on 2-D MOF nanosheets, MOF particles didn't grow big enough to contact with each other to form a continuous layer. Fig. S2 (c,d) showed there were still defects on MOF layer after 6 cycles L-b-L growth and the gas separation results (Fig. S3a) also proved that there was no selectivity for ZIF-8 composite membrane after six and less L-b-L growth.

In order to study the function of 2-D MOF seeds, we prepared ZIF-8 composite membrane on hydrolysis PAN membrane without seeds via 10-cycles of L-b-L method. As is shown in Fig. S4a,b, many obvious cracks occurred due to the bad adhesion between MOF layer with polymer substrate. These cracks resulted in minimal gas selectivity for the ZIF-8 composite membrane (Fig. S3b).
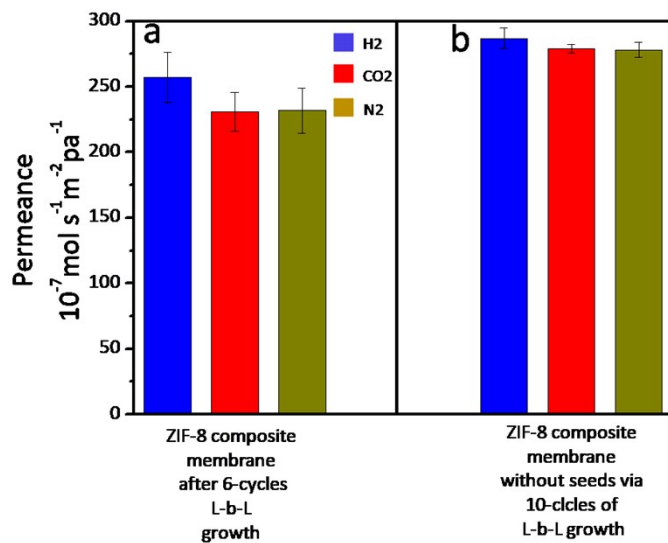
Fig. S3. Gas permeance of ZIF-8 composite membrane after 6-cycles L-b-L growth (a) and ZIF-8 composite membrane without seeds via 10-cycles of L-b-L growth (b) in 0.1 MPa at room temperature.
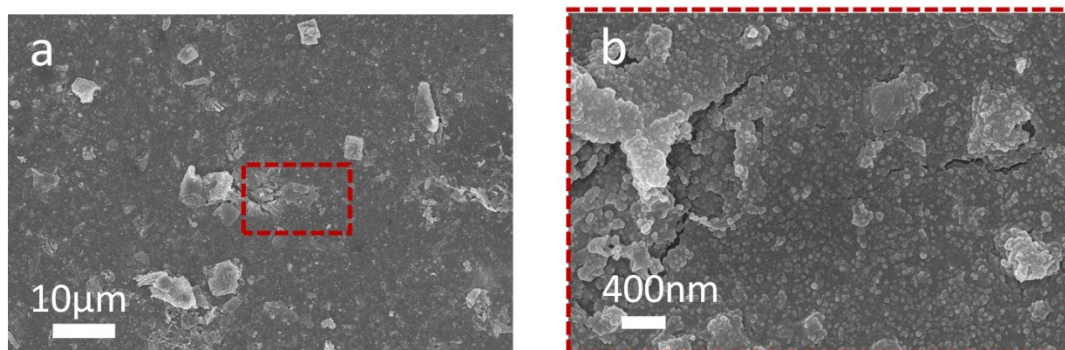

Fig. S4. ZIF-8 composite membrane without seeds via 10-clcles of L-b-L growth (a,b).

3 Gas permeation tests

Single gas permeations were tested using a constant feed/sweep pressure instrument (Fig. S5) at 25 °C, and the driving force across the membranes was provided by a pressure gradient. The gas volume and time required for permeating a membrane were measured by a bubble flow meter. More than 3 membranes were tested for a single gas permeation to calculated the average. The permeation flux J_i (mol m^{-2} Pa^{-1} s^{-1}) of all the gases was calculated using the membrane area A(m^2), the transmembrane partial pressure difference Δp_i (Pa), the volume of permeating gas V_i (mol), and the time t_i (s), as were shown in Equation (1); The ideal selectivity α_{ij} of two gases (i and j) was calculated as the ratio of their permeances[7] shown in Equation (2).

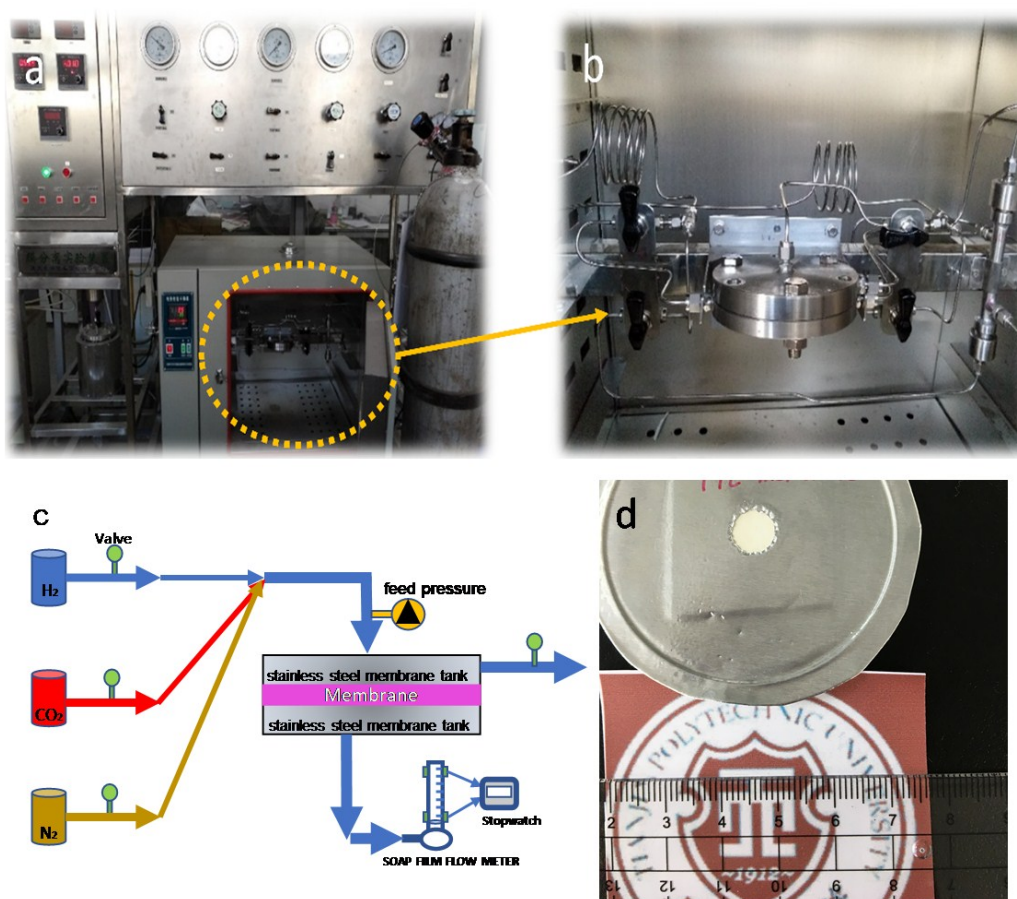$$J_i = \frac{V_i}{A \cdot \Delta P_i \cdot t_i} \quad (1) \qquad \alpha_{ij} = \frac{J_i}{J_j} \quad (2)$$

Fig. S5. The photos of feed/sweep pressure instrument gas separation equipment: the overall picture (a); the details inside (b); the schematic diagram of gas permeation measurement (c); and the membrane covered by an aluminum foil tape for test (d).

Table S1 Comparison of the gas-separation performance of the thin MOF membrane on various supports

Membrane	Substrate	Thickness (x 100 nm)	H_2 permeance $\times 10^{-7}$ mol m^{-2}s^{-1} Pa^{-1}	Selectivity		Ref.
				H_2/CO_2	H_2/N_2	
ZIF-8	BPPO hollow fiber	2	20.5	12.8	9.7	[35]
ZIF-8	PVDF hollow fiber	<10	201	7	7.8	[17]
ZIF-8	PSF	500	2	NA	12.4	[16]
ZIF-8	Nylon hollow fiber	25	11.3	NA	4.6	[36]
ZIF-8	Nylon hollow fiber	160	126.2	NA	3.7	[38]
ZIF-8	PVDF	0.9	119	NA	22.4	[37]
CuBTC	PVDF	30	20	8.1	6.5	[39]
ZIF-8	PVDF hollow fiber	400	24.4	12.2	14.3	[40]
ZIF-7		300	13.3	16.3	18.3	
CuBTC		500	84.6	7.3	5.9	
ZIF-8	ZIF-8/2-D MOF/PAN	4.4	9.5	13	22.6	This work

References

7. P. Neelakanda, E. Barankova, K.V. Peinemann, *Micropor. Mesopor. Mat.,* 2016, **220**, 215-219.

16. F. Cacho-Bailo, B. Seoane, C. Téllez, J. Coronas, *J. Membr. Sci.,* 2014, **464**, 119-126.

17. J. Hou, P.D. Sutrisna, Y. Zhang, V. Chen, *Angew. Chem. Int. Ed.,* 2016, **55**, 3947-3951.

24. Y. Peng, Y.S.Li, Y.J.Ban, H.Jin, W.M.Jin, X.L.Liu, W.S.Yang, *Science,* 2014, **346**, 1356.

26. G. Zhang, H. Yan, S. Ji, Z. Liu, *J. Membr. Sci.*, 2007, **292**, 1-8.

35.E. Shamsaei, Z.X. Low, X. Lin, A. Mayahi, H. Liu, X. Zhang, J.L. Zhe, H. Wang, *Chem. Commun.,* 2015, **51**, 11474-11477.

36. H. Ming, J. Yao, L. Li, Z. Zhong, F. Chen, H. Wang, *Micropor. Mesopor. Mat.* 2013, **179**, 10-16.

37. W. Li, P. Su, Z. Li, Z. Xu, F. Wang, H. Ou, J. Zhang, G. Zhang, E. Zeng, *Nat. Commun.,* 2017, **8**, 406.

38. J. Yao, D. Dong, D. Li, L. He, G. Xu, H. Wang, *Chem. Commun.*, 2011, **47**, 2559-2561.

39. Y. Mao, J. Li, W. Cao, Y. Ying, L. Sun, X. Peng, *ACS Appl. Mater. Interfaces.,* 2104, **6**, 4473-4479.

30. W. Li, Q. Meng, C. Zhang, G. Zhang, *Chem-Eur J.*, 2015, **21**, 7224-7230.